

This document is the unedited Author's version of a Submitted Work that was subsequently accepted for publication in Crystal Growth & Design, copyright © American Chemical Society after peer review. To access the final edited and published work see <https://doi.org/10.1021/acs.cgd.1c00875>. Access to this work was provided by the University of Maryland, Baltimore County (UMBC) ScholarWorks@UMBC digital repository on the Maryland Shared Open Access (MD-SOAR) platform.

Please provide feedback

Please support the ScholarWorks@UMBC repository by emailing [scholarworks-group@umbc.edu](mailto:scholarworks-group@umbc.edu) and telling us what having access to this work means to you and why it's important to you. Thank you.

# Low-temperature dopant-assisted crystallization of HfO<sub>2</sub> thin films

Theodosia Gougousi

Department of Physics, UMBC, Baltimore, MD 21250, USA.

email: [gougousi@umbc.edu](mailto:gougousi@umbc.edu)

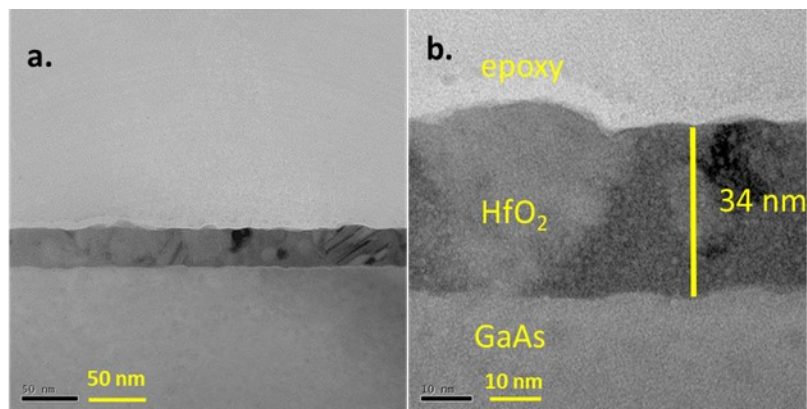
We have studied the thermal atomic layer deposition (ALD) of HfO<sub>2</sub> on native and chemical oxide GaAs(100) surfaces using the amide precursors tetrakis ethymethyl amino hafnium and tetrakis dimethylamino hafnium. Bright-field and HRTEM data for *as-prepared* HfO<sub>2</sub> films deposited on both GaAs(100) oxide surfaces show that the films are polycrystalline and contain several large grains of the order of the film thickness and numerous smaller ones. X-ray diffraction confirms the presence of small crystallites that can be classified in forms other than monoclinic while control films deposited on native oxide Si(100) surfaces are amorphous. Thermally treated films deposited on both Si and GaAs contain mainly monoclinic grains. Gallium and arsenic oxides are known to bubble through the growing HfO<sub>2</sub> film so that at any point during the ALD process, there is mixing of the various III-V oxides in the film. These oxides seem to stabilize the various HfO<sub>2</sub> polymorphs during low-temperature thermal ALD allowing control of the film microstructure via the deposition process.

Keywords: Atomic Layer Deposition, crystallization, hafnium oxide, nanograins, amide ligand

## Highlights

- Atomic Layer Deposition of  $\text{HfO}_2$  on native and chemical oxide GaAs(100) surfaces results in the formation of polycrystalline films.
- The as-deposited film contains monoclinic, tetragonal, and/or cubic phases.
- Thermally treated films comprise almost exclusively of monoclinic grains.
- Mixing of gallium and arsenic oxides in the growing film is linked to the observed film crystallization at low temperatures.

## Graphical abstract



## Introduction

Transition metal oxides have been the subject of intense study due to their use in many technologies such as nanoelectronics, sensors, photocatalysis, etc., both in amorphous and crystalline forms.  $\text{HfO}_2$  can be found in a variety of phases such as cubic, tetragonal, monoclinic, and more recently the orthorhombic<sup>1-4</sup>. For thin films which are the subject of this proposal, crystallization usually proceeds by nucleation in the tetragonal phase due to the surface energy effect but the monoclinic phase takes over and appears the most dominant<sup>5,6</sup>. The most common approach to inducing crystallization is thermal treatment and there have been numerous examples in the literature for the types of films that are the subject of this work<sup>7-15</sup>. In most cases, such a process is not controlled, and thermodynamics tends to determine the abundance of the various phases present in the film. Other approaches such as laser heating have been proposed to provide more localized control of the process, but they have very low throughput<sup>1,16</sup>. There are instances where the as-deposited film is polycrystalline, for example,  $\text{HfO}_2$  films prepared by reactive sputtering are monoclinic at temperatures around 150°C.<sup>17</sup> Other approaches used to produce crystalline materials such as ball milling and sol-gel are producing mainly powders<sup>18-23</sup>.

$\text{HfO}_2$  has been studied extensively as a potential replacement for  $\text{SiO}_2$  in gate oxide applications (high-k dielectrics), and in this context, it is usually preferred to be amorphous. Approaches that include the formation of nanolaminate structures have been employed to retain the amorphous nature of the films during thermal treatment<sup>24-30</sup>. However, certain crystalline phases have a higher dielectric constant (cubic:  $k \sim 29$ , tetragonal:  $k \sim 70$ , and monoclinic:  $k \sim 16$ ), so stabilization of these phases is not undesirable<sup>2,31</sup>. For sensing applications, such as detection of

CO<sup>32,33</sup>, NO<sub>2</sub><sup>34</sup>, and H<sub>2</sub><sup>35</sup>, HfO<sub>2</sub> polycrystalline powders are preferred. Doping has been demonstrated to assist in the stabilization of the ferroelectric and antiferroelectric phases<sup>36–39</sup>.

Atomic Layer Deposition (ALD) was initially introduced as Atomic Layer Epitaxy (ALE) and led to the formation of polycrystalline films mainly for electroluminescent displays<sup>40</sup>. However, these original processes used inorganic precursors such as halides and operated at temperatures over 400°C. Most state-of-the-art ALD processes utilize metal-organic precursors that decompose at such temperatures and the ALD window for these processes can be found at temperatures below 300°C. At these temperatures, the vast majority of the as-deposited ALD films are amorphous<sup>41</sup>. A notable exception is ZnO which is polycrystalline even at ALD temperatures as low as 100°C<sup>42,43</sup>. Miikkulainen et al. list several metal-organic HfO<sub>2</sub> ALD processes that produce polycrystalline films at 300–350°C<sup>41</sup>. One should keep in mind that film thickness is an important parameter. HfO<sub>2</sub> films with thickness around 100 nm are known to crystallize partially at 250°C and in general, the crystallization onset temperature is inversely proportional to the film thickness<sup>4,5,10,13,30,44–47</sup>. For example, Kukli et al. demonstrated thickness-dependent crystallization for HfO<sub>2</sub> films deposited from tetrakis ethylmethylamino hafnium (TEMAHf) and H<sub>2</sub>O at 250°C: 5 nm film are amorphous, 30 nm barely crystalline, and for 45 nm films the presence of crystallization is evident<sup>48</sup>. Boscke et al. demonstrated that films below 7 nm remain amorphous up to 425°C<sup>5</sup>. Recently Hsain et al. in a very detailed study have shown that 30 nm HfO<sub>2</sub> films produced from tetrakis dimethylamino hafnium (TDMAHf) and H<sub>2</sub>O at 270°C remain amorphous until 386°C<sup>4</sup> and Gusev et al. have also demonstrated the inverse dependence of crystallization temperature on film thickness<sup>49</sup>.

In this manuscript, we will demonstrate that HfO<sub>2</sub> films with thicknesses from 6 to 34 nm deposited at 250–275°C on GaAs oxide surfaces are polycrystalline and contain a variety of

crystalline phases. This grain stabilization will be linked to the mixing of gallium and arsenic oxides in the film. These oxides act as stabilizing agents for the formation of fine HfO<sub>2</sub> grains.

#### Experiment:

Two GaAs(100) surface preparations were examined; native and chemical oxides. Native oxide surfaces were cleaned in acetone (5 min), methanol (5 min), rinsed in deionized water (DI) water (5 min), and dried with N<sub>2</sub>. For the chemical oxides, the initial step involved soaking of the as-received GaAs(100) in J. T. Baker 100 solution<sup>50</sup> for 5 minutes, followed by 5 minutes DI water rinse, 3 min etch in NH<sub>4</sub>OH, a quick wash in DI water and N<sub>2</sub> blow dry. Growth of the chemical oxide layer was accomplished by immersing the GaAs surfaces in aqueous H<sub>2</sub>O<sub>2</sub> solution at ~ 45°C followed by a DI water rinse and N<sub>2</sub> blow dry. These surfaces are referred to as “CO GaAs” in the remainder of this manuscript. Since chemical oxide surfaces were prepared well in advance, before use they were cleaned in acetone (5 min), methanol (5 min), rinsed in DI water (5 min), and dried with N<sub>2</sub>.

The depositions were performed in a home-built flow-tube type ALD reactor. Two thermal ALD processes involved precursors from the same amine family, TDMAHf and TEMA Hf, were used. H<sub>2</sub>O was the oxidizer in both cases. The deposition temperature was 250°C for TEMA Hf and 275°C for TDMAHf. Some of the samples were thermally treated using a MILA 3000 rapid thermal annealer in Argon ambient. Native oxide Si(100) companion samples were included in all depositions. These samples were cleaned in JTB for 5 min, followed by a 5 min DI rinse and N<sub>2</sub> blow dry.

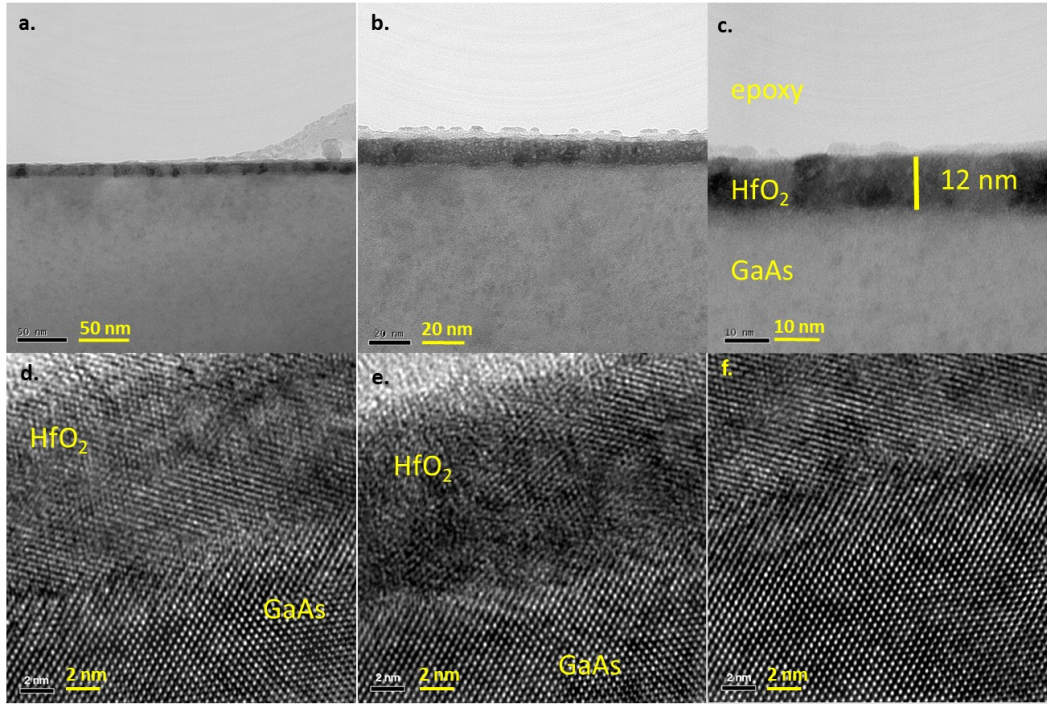


**Figure 1.** (a)-(c) Bright field and (d)-(f) High Resolution Transmission Electron Microscopy data for a 12 nm *as-deposited* HfO<sub>2</sub> film from TEMA<sub>4</sub>Hf and H<sub>2</sub>O at 250°C on native oxide GaAs(100) surfaces. The presence of crystallites is evident in all images. Some of the grain span the film thickness but many smaller ones are clearly visible. The film has not been subjected to post deposition thermal treatment.

Film thickness was measured routinely on the companion Si samples using an alpha SE spectroscopic ellipsometer (Wollam). Bright-field and high-resolution transmission electron microscopy (HRTEM) data were taken by TEM Lab services. X-ray Diffraction data were obtained using a Bruker D8 Advance powder diffractometer with a Cu radiation source ( $\lambda=1.54060\text{\AA}$ )

## Results:

Figures 1 and 2 show bright field and HRTEM data for *as-prepared* 12 nm and 34 nm of HfO<sub>2</sub> respectively deposited on native oxide GaAs(100) at 250°C from TEMA<sub>4</sub>Hf and H<sub>2</sub>O. As



received GaAs(100) surfaces are usually covered by  $\sim 2$  nm of native oxides. In addition to confirmation of the removal of  $\sim 2$  nm of native oxides during the deposition, the data reveal that the **as-deposited** film is polycrystalline and contains several large grains (of the order of the film thickness) and numerous small crystallites (2-10 nm) as evidenced by the spots in the bright field images and confirmed by the high-resolution data included in the figure.

To clarify the role of the GaAs(100) substrate in the observed  $\text{HfO}_2$  film structure an additional set of films of thickness 6 and 24 nm was grown on GaAs(100) surfaces that were chemically oxidized. The chemical oxide layer thickness was measured at  $\sim 4.6$  nm (Figure 3), more than

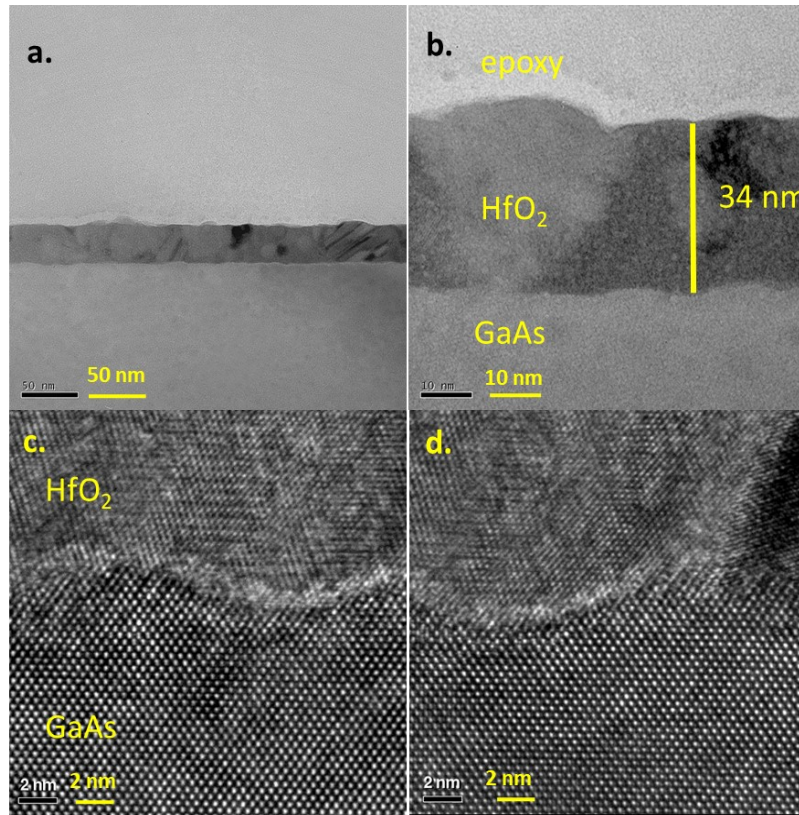


**Figure 2.** (a),(b) Bright field and (c)-(d) High Resolution Transmission Electron Microscopy data for a 34 nm **as-deposited**  $\text{HfO}_2$  film from  $\text{TEMAHf}$  and  $\text{H}_2\text{O}$  at  $250^\circ\text{C}$  on native oxide GaAs(100) surfaces. The presence of crystallites is evident in all images. Some of the grain span the film thickness but many smaller ones are clearly visible too. The film has not been subjected to post deposition thermal treatment.

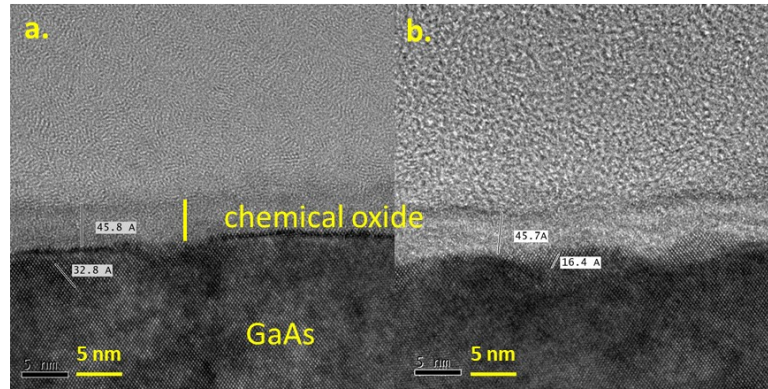


**Figure 3.** (a),(b) High Resolution Transmission Electron Microscopy data for a chemical oxide (CO) GaAs(100) sample. The thickness of the CO layer is  $\sim 4.6$  nm.

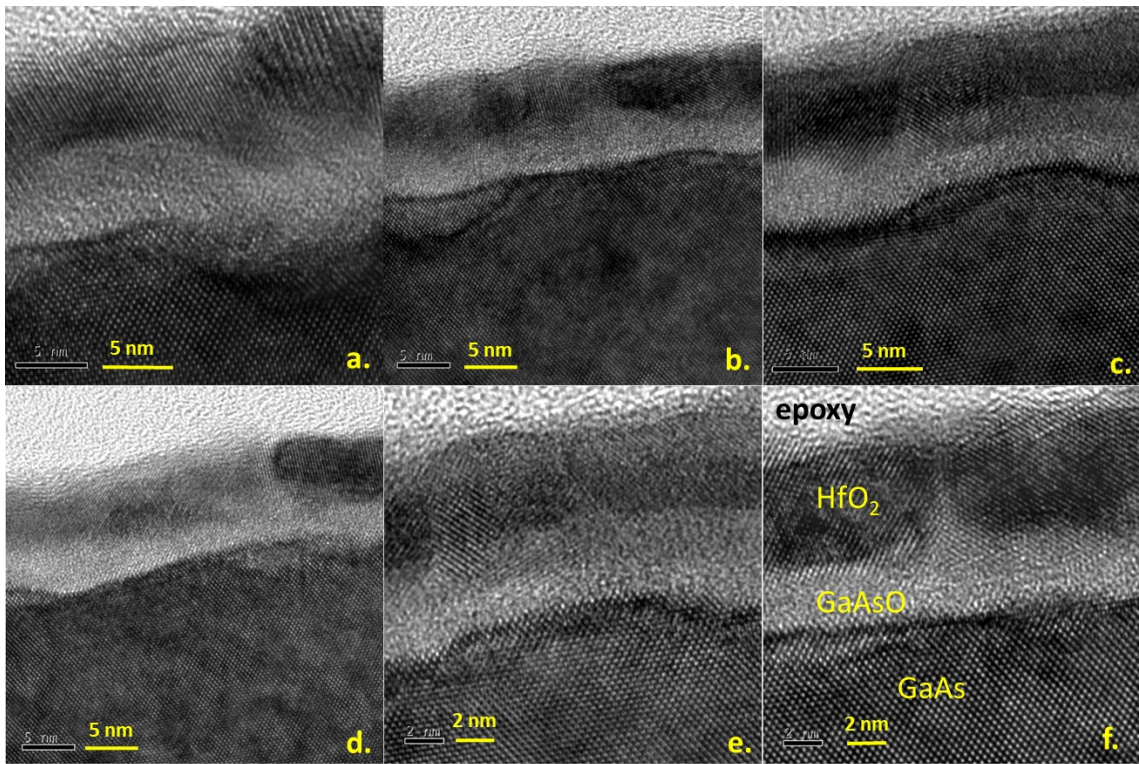


**Figure 4.** (a)-(f) High Resolution Transmission Electron Microscopy data for a 6 nm  $\text{HfO}_2$  film deposited from TEMAHf and  $\text{H}_2\text{O}$  at  $250^\circ\text{C}$  on 4.6 nm chemical oxide GaAs(100) surfaces. The presence of crystallites is evident in all images. The film has not been subjected to post deposition thermal treatment.



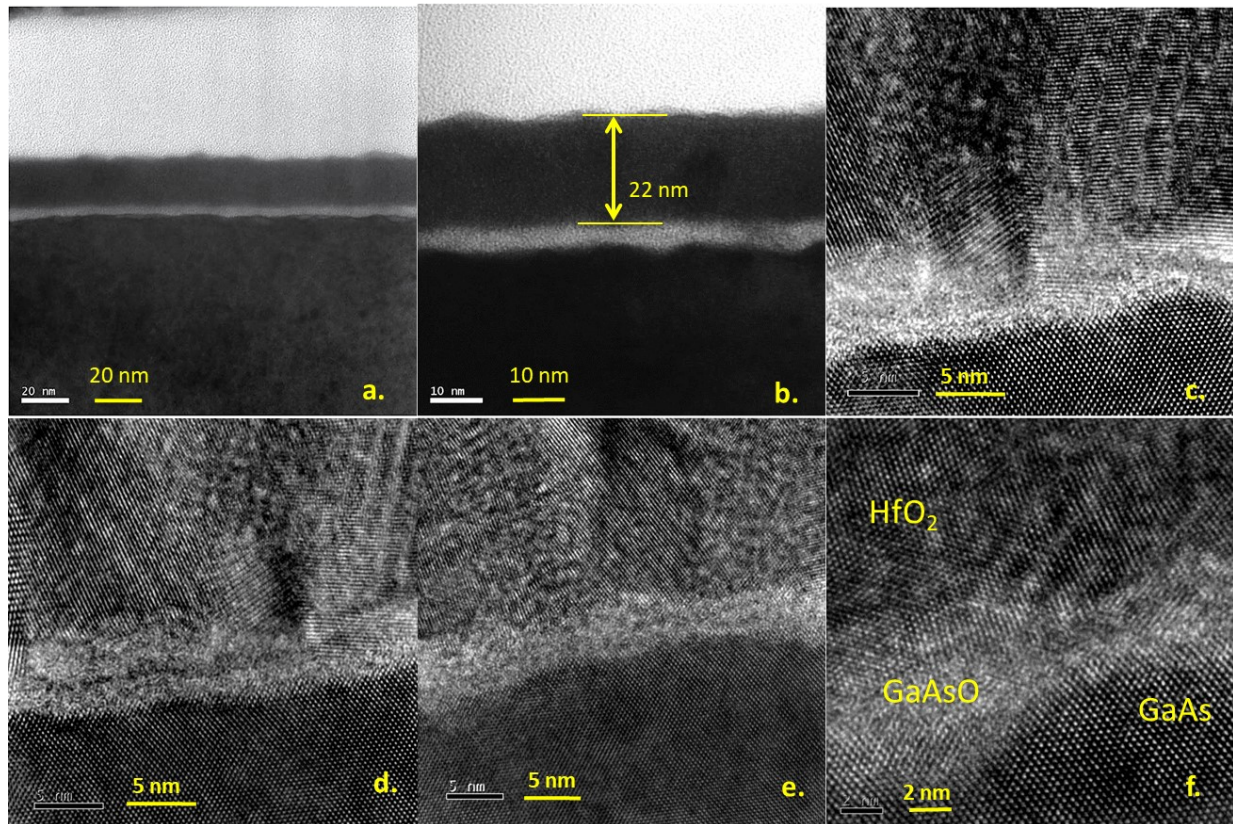


**Figure 5.** (a)-(b) Bright field and (c)-(f) High Resolution Transmission Electron Microscopy data for a 22 nm HfO<sub>2</sub> film deposited from TEMAHf and H<sub>2</sub>O at 250°C on 4.6 nm chemical oxide GaAs(100) surfaces. The film has not been subjected to post deposition thermal treatment.

twice the thickness of the native oxides. GaAs chemical oxides are similar in composition to the native oxides<sup>51</sup>. Depositions of ~6 nm of HfO<sub>2</sub> from the same precursors as before showing the formation of a polycrystalline film while ~2 nm of the chemical oxide layer is still detectable at the interface (Figure 4). The importance of this is twofold. First, there is no direct contact of the HfO<sub>2</sub> layer with the GaAs substrate and even in the 6 nm as-deposited film the presence of several crystallites is detected. It is well established that HfO<sub>2</sub> films of such low thickness remain amorphous even after they are subjected to thermal treatment<sup>31,36,38,48,49</sup>. The 24 nm as-deposited film (Figure 5) is also polycrystalline and shows the presence of some of the chemical oxides at the interface. A piece of this sample was also annealed for 3 min at 700°C in Argon in a rapid

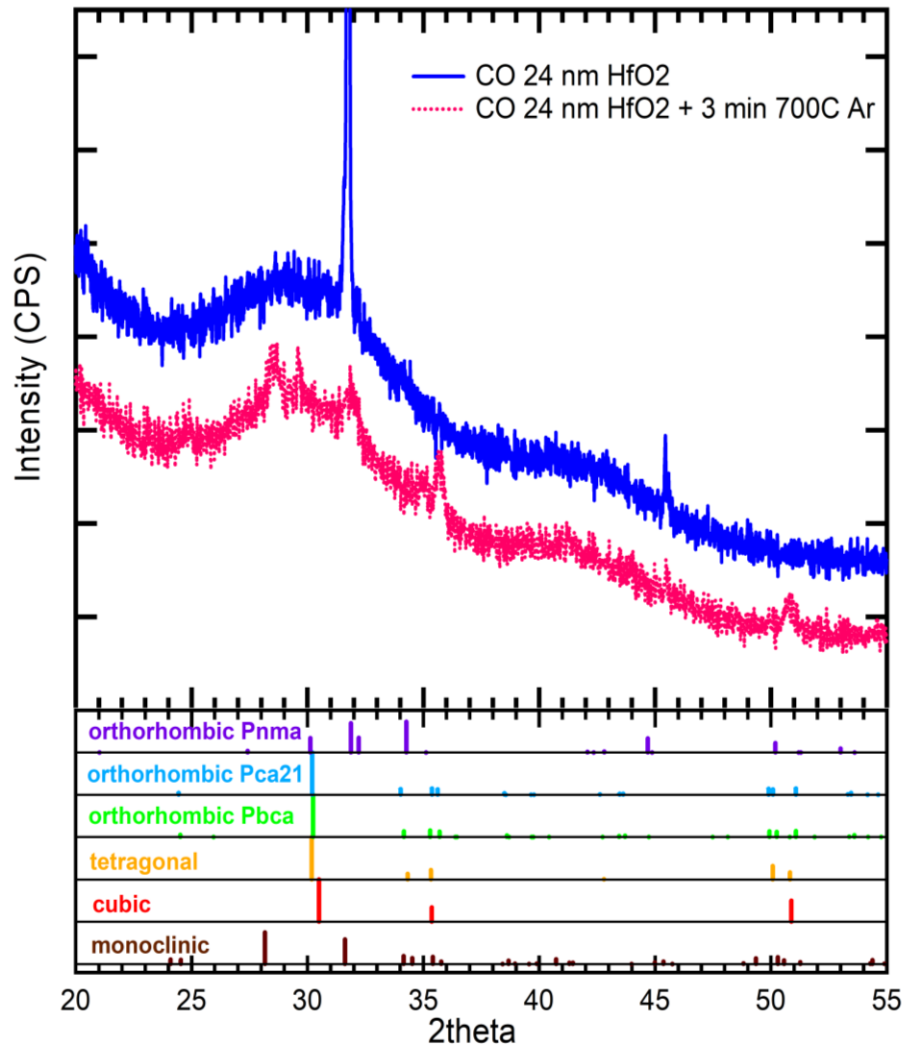


**Figure 6.** XRD for 22 nm HfO<sub>2</sub> from TEMAHf and H<sub>2</sub>O deposited on chemical oxide (CO) GaAs (100) at 250°C. The as-deposited films on CO GaAs shows the presence of grains from different polymorphs grains. After thermal treatment for 3 min at 700°C both the film is composed primarily from monoclinic grains.

thermal annealer. Subsequently, the structure of the as-deposited and the thermally treated sample was examined by x-ray diffraction (XRD) and the results are shown in Figure 6. Patterns for all known HfO<sub>2</sub> polymorphs are included in the figure. The sharp feature at  $2\theta \approx 31.7^\circ$  is due to the GaAs substrate and should be ignored. The presence of the broad feature at  $2\theta = 25$ - $35^\circ$  in the spectrum for the as-deposited film confirms the HRTEM data from Figure 5 that the

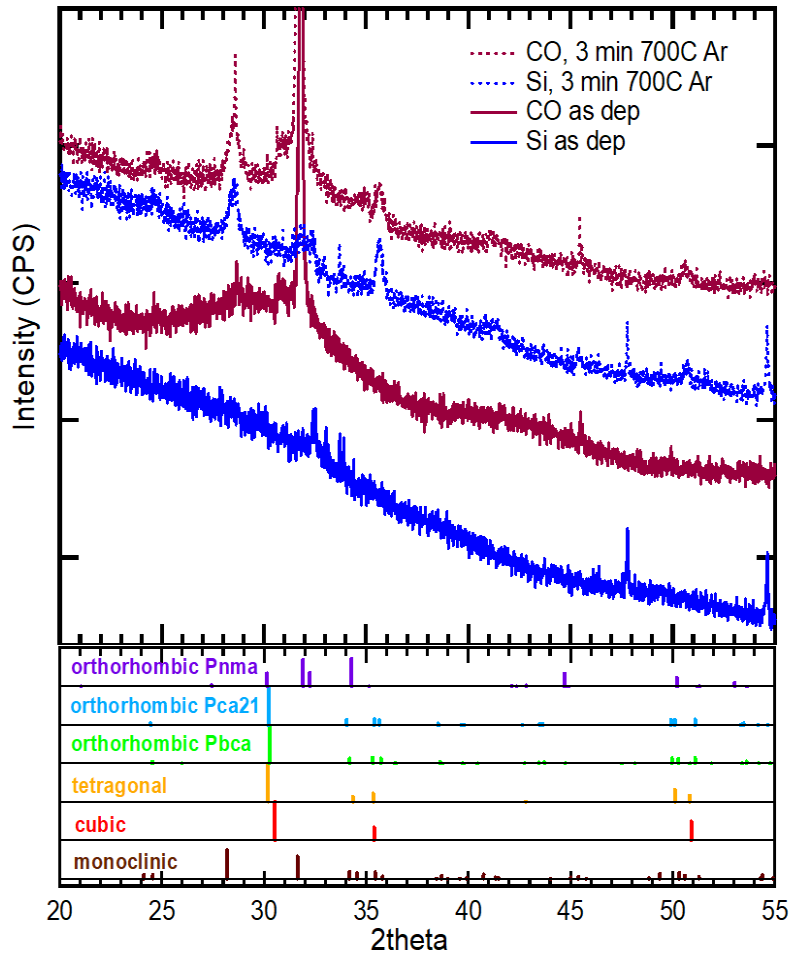


**Figure 7.** XRD for 30 nm HfO<sub>2</sub> from TDMAHf and H<sub>2</sub>O deposited simultaneously on chemical oxide (CO) GaAs (100) and native oxide Si(100) at 275°C. As-deposited films on CO GaAs show the presence of a variety of grains. After thermal treatment for 3 min at 700°C both the Co GaAs and Si films show the presence of monoclinic grains.

film is polycrystalline and contains many small crystallites that can be assigned to several different types of polymorphs. In the same spectral region, the features become sharper after the thermal treatment and are mostly consistent with the presence of monoclinic grains.

Subsequently, we deposited ~ 30 nm at the ALD optimal temperature of 275°C both on chemical oxide GaAs(100) surfaces and native oxide Si(100) as a control sample using TDMAHf and H<sub>2</sub>O. The XRD patterns for the as-deposited films on Si and GaAs and their thermally treated

counterparts are shown in Figure 7. The as-deposited film on CO GaAs shows a broad peak at  $2\theta=25-35^\circ$  that is compatible with the presence of a large number of small size monoclinic, tetragonal and cubic crystallites, similar to the sample in Figure 6. However, the as-deposited film on Si is predominantly amorphous as evidenced by the broad structureless peak. Overlaid on the background, there are some features compatible with monoclinic  $\text{HfO}_2$  in agreement with earlier work<sup>45,46,48</sup>. After the thermal treatment, the film deposited on Si shows extensive crystallization in the monoclinic and the one deposited on CO GaAs shows several peaks that can be classified as monoclinic and a couple that can be assigned to more than one other polymorph.

## Discussion

The ALD of  $\text{HfO}_2$  and  $\text{TiO}_2$  on III-V surfaces such as GaAs(100) and InAs (100) surfaces using amide precursors has been studied extensively. One of the highlights of these processes is the so-called interface cleaning reaction that leads to the gradual consumption of the surface native oxides and results in the formation of a sharp metal oxide/III-V semiconductor interface<sup>52-60</sup>. It has been demonstrated that this interface cleaning reaction continues after the native oxides have been covered by a monolayer of the growing film at which point there is no direct contact of the precursor and/or the ALD reaction by-products with the surface native oxides. Instead, it has been shown that the removal is accomplished because the surface native oxides transport to the surface of the growing ALD oxide layer where they react with the precursor to form volatile by-products that are removed. So there is always mixing of the various III-V oxides in the growing ALD film but because of the removal mechanism, the final film has very low impurity content

<sup>53,57,61,62</sup>. We hypothesize that the presence of these gallium and arsenic oxides in the bulk of the growing film leads to stabilization of the grains as evidenced by the HRTEM and XRD data.

The as-deposited HfO<sub>2</sub> films contain a variety of polymorphs and the presence of polymorphs other than monoclinic is confirmed. It is known that for HfO<sub>2</sub> the surface area affects the prevalence of the various polymorphs and for coarse-grained materials, the monoclinic phase is thermodynamically the most stable at room temperature <sup>6</sup>. However, the presence of tetragonal phases is also possible for fine-grain (high surface area) films formed at low temperatures as is the case for the films produced by the thermal ALD process we have used. Unlike GaAs surfaces, XRD data indicate that the HfO<sub>2</sub> films deposited on Si substrates under identical conditions are mainly amorphous with some monoclinic features in agreement with earlier observations <sup>45,46,48</sup>. The difference in the structure observed between the films deposited on GaAs and Si substrates under similar conditions indicates the existence of a stabilization mechanism in which the surface is involved. ALD was initially called ALE so an epitaxial type of process cannot be excluded. While the films deposited on the native oxide result in the formation of a sharp HfO<sub>2</sub>/GaAs interface due to the interface cleaning reaction, for the films deposited on the thicker chemical oxide-covered GaAs surfaces there is about 2 nm of the chemical oxide left at the interface even after the 22 nm film deposition. For these experiments, at no point during the film growth, there is direct contact of the HfO<sub>2</sub> with the single crystal substrate. Based on the above, the possibility of an epitaxial type of growth is rejected. The other possibility is that the gallium and arsenic oxides are responsible for the nanograin stabilization. The exact mechanism is yet to be determined but it is clear from the comparison between the Si and the GaAs films that the presence of the gallium and arsenic affects

significantly the film morphology. For both surfaces, high-temperature anneals result in the coarsening of the HfO<sub>2</sub> films and the stabilization of the monoclinic form as expected.

Dopant-assisted grain stabilization is well-known. For example, dopants such as Si, Ge, etc. are known to help in the stabilization of the ferroelectric phase of HfO<sub>2</sub><sup>36–39</sup>. So in this case, the presence of ~2 nm of gallium and arsenic oxides on the starting surface is sufficient to provide a pathway to control and optimize the film structure using a low-temperature deposition process such as thermal ALD. Furthermore, since the arsenic and gallium oxides react with the amide precursor to form volatile by-products, they do not affect the film composition. As a result, this approach facilitates the integration of ALD dielectrics with flexible substrates and hybrid architectures which is highly desirable from a technological standpoint<sup>16,63,64</sup>.

## Conclusions

The ALD of HfO<sub>2</sub> on GaAs native and chemical oxide surfaces leads to the formation of polycrystalline films that may contain cubic and tetragonal in addition to monoclinic grains. By contrast, films deposited on Si(100) using a similar process are mainly amorphous. This HfO<sub>2</sub> film crystallization when deposited on GaAs oxide surfaces is linked to the mixing of the gallium and arsenic oxide in the growing film that leads to the formation of a fine-grained thin film. Thermal treatment of films deposited both on GaAs and Si surfaces results in the detection of predominantly monoclinic grains.



#### Acknowledgments:

The author thanks Peter Zavalij from the University of Maryland, X-ray Crystallographic Center for assistance with the XRD data and helpful discussions.

## References:

- (1) Tabata, T. Nucleation and Crystal Growth in HfO<sub>2</sub> Thin Films by UV Nanosecond Pulsed Laser Annealing. *Appl. Phys. Express* **2019**, *13* (1), 015509. <https://doi.org/10.7567/1882-0786/ab5ce2>.
- (2) Zhao, X.; Vanderbilt, D. First-Principles Study of Structural, Vibrational, and Lattice Dielectric Properties of Hafnium Oxide. *Physical Review B* **2002**, *65* (23). <https://doi.org/10.1103/PhysRevB.65.233106>.
- (3) Zhou, B.; Shi, H.; Zhang, X. D.; Su, Q.; Jiang, Z. Y. The Simulated Vibrational Spectra of HfO<sub>2</sub> Polymorphs. *Journal of Physics D: Applied Physics* **2014**, *47* (11), 115502. <https://doi.org/10.1088/0022-3727/47/11/115502>.
- (4) Hsain, H. A.; Lee, Y.; Parsons, G.; Jones, J. L. Compositional Dependence of Crystallization Temperatures and Phase Evolution in Hafnia-Zirconia (Hf<sub>x</sub>Zr<sub>1-x</sub>)O<sub>2</sub> Thin Films. *Appl. Phys. Lett.* **2020**, *116* (19), 192901. <https://doi.org/10.1063/5.0002835>.
- (5) Böске, T. S.; Govindarajan, S.; Kirsch, P. D.; Hung, P. Y.; Krug, C.; Lee, B. H.; Heitmann, J.; Schröder, U.; Pant, G.; Gnade, B. E.; Krautschneider, W. H. Stabilization of Higher- $\kappa$  Tetragonal HfO<sub>2</sub> by SiO<sub>2</sub> Admixture Enabling Thermally Stable Metal-Insulator-Metal Capacitors. *Appl. Phys. Lett.* **2007**, *91* (7), 072902. <https://doi.org/10.1063/1.2771376>.
- (6) Navrotsky, A. Thermochemical Insights into Refractory Ceramic Materials Based on Oxides with Large Tetravalent Cations. *J. Mater. Chem.* **2005**, *15* (19), 1883–1890. <https://doi.org/10.1039/B417143H>.
- (7) Jung, J.-W.; Kim, G.-Y.; Lee, N.-W.; Ryu, W.-H. Low-Temperature Synthesis of Tetragonal Phase of Hafnium Oxide Using Polymer-Blended Nanofiber Precursor. *Applied Surface Science* **2020**, *533*, 147496. <https://doi.org/10.1016/j.apsusc.2020.147496>.
- (8) Puthenkovilakam, R.; Lin, Y.-S.; Choi, J.; Lu, J.; Blom, H.-O.; Pianetta, P.; Devine, D.; Sandler, M.; Chang, J. P. Effects of Post-Deposition Annealing on the Material Characteristics of Ultrathin HfO<sub>2</sub> Films on Silicon. *Journal of Applied Physics* **2004**, *97* (2), 023704. <https://doi.org/10.1063/1.1831543>.
- (9) Ushakov, S. V.; Navrotsky, A.; Yang, Y.; Stemmer, S.; Kukli, K.; Ritala, M.; Leskelä, M. A.; Fejes, P.; Demkov, A.; Wang, C.; Nguyen, B.-Y.; Triyoso, D.; Tobin, P. Crystallization in Hafnia- and Zirconia-Based Systems. *physica status solidi (b)* **2004**, *241* (10), 2268–2278. <https://doi.org/10.1002/pssb.200404935>.
- (10) Zhang, L.; Zhang, J.; Jiao, H.; Bao, G.; Wang, Z.; Cheng, X. Thickness-Dependent Surface Morphology and Crystallization of HfO<sub>2</sub> Coatings Prepared with Ion-Assisted Deposition. *Thin Solid Films* **2017**, *642*, 359–363. <https://doi.org/10.1016/j.tsf.2017.10.010>.
- (11) Schaeffer, J.; Edwards, N. V.; Liu, R.; Roan, D.; Hradsky, B.; Gregory, R.; Kulik, J.; Duda, E.; Contreras, L.; Christiansen, J.; Zollner, S.; Tobin, P.; Nguyen, B.-Y.; Nieh, R.; Ramon, M.; Rao, R.; Hegde, R.; Rai, R.; Baker, J.; Voight, S. HfO<sub>2</sub> Gate Dielectrics Deposited via Tetrakis Diethylamido Hafnium. *J. Electrochem. Soc.* **2003**, *150* (4), F67. <https://doi.org/10.1149/1.1554729>.

- (12) Biswas, D.; Singh, M. N.; Sinha, A. K.; Bhattacharyya, S.; Chakraborty, S. Effect of Excess Hafnium on HfO<sub>2</sub> Crystallization Temperature and Leakage Current Behavior of HfO<sub>2</sub>/Si Metal-Oxide-Semiconductor Devices. *Journal of Vacuum Science & Technology B* **2016**, *34* (2), 022201. <https://doi.org/10.1116/1.4941247>.
- (13) Fu, W.-E.; Chang, Y.-Q. Layer Structure Variations of Ultra-Thin HfO<sub>2</sub> Films Induced by Post-Deposition Annealing. *Applied Surface Science* **2011**, *257* (17), 7436–7442. <https://doi.org/10.1016/j.apsusc.2011.02.132>.
- (14) Ho, M.-Y.; Gong, H.; Wilk, G. D.; Busch, B. W.; Green, M. L.; Voyles, P. M.; Muller, D. A.; Bude, M.; Lin, W. H.; See, A.; Loomans, M. E.; Lahiri, S. K.; Räisänen, P. I. Morphology and Crystallization Kinetics in HfO<sub>2</sub> Thin Films Grown by Atomic Layer Deposition. *Journal of Applied Physics* **2003**, *93* (3), 1477–1481. <https://doi.org/10.1063/1.1534381>.
- (15) Jõgiaas, T.; Kull, M.; Seemen, H.; Ritslaid, P.; Kukli, K.; Tamm, A. Optical and Mechanical Properties of Nanolaminates of Zirconium and Hafnium Oxides Grown by Atomic Layer Deposition. *Journal of Vacuum Science & Technology A* **2020**, *38* (2), 022406. <https://doi.org/10.1116/1.5131563>.
- (16) Chen, C.; Yang, H.; Yang, Q.; Chen, G.; Chen, H.; Guo, T. Low-Temperature Solution-Processed Flexible Metal Oxide Thin-Film Transistors via Laser Annealing. *J. Phys. D: Appl. Phys.* **2019**, *52* (38), 385105. <https://doi.org/10.1088/1361-6463/ab2c51>.
- (17) Pi, N.-W.; Zhang, M.; Jiang, J.; Belosludtsev, A.; Vlček, J.; Houška, J.; Meletis, E. I. Microstructure of Hard and Optically Transparent HfO<sub>2</sub> Films Prepared by High-Power Impulse Magnetron Sputtering with a Pulsed Oxygen Flow Control. *Thin Solid Films* **2016**, *619*, 239–249. <https://doi.org/10.1016/j.tsf.2016.10.059>.
- (18) Chain, C. Y.; Damonte, L. C.; Ferrari, S.; Muñoz, E.; Torres, C. R.; Pasquevich, A. F. PAC Study in the HfO<sub>2</sub>–SiO<sub>2</sub> System. *Journal of Alloys and Compounds* **2010**, *495* (2), 527–531. <https://doi.org/10.1016/j.jallcom.2009.10.167>.
- (19) Takacs, L. Ball Milling-Induced Combustion in Powder Mixtures Containing Titanium, Zirconium, or Hafnium. *Journal of Solid State Chemistry* **1996**, *125* (1), 75–84. <https://doi.org/10.1006/jssc.1996.0267>.
- (20) Hsu, C.-C.; Liu, Y.-N.; Ma, H.-K. Effect of the Zr<sub>0.5</sub>Hf<sub>0.5</sub>CoSb<sub>1-x</sub>Sn<sub>x</sub>/HfO<sub>2</sub> Half-Heusler Nanocomposites on the ZT Value. *Journal of Alloys and Compounds* **2014**, *597*, 217–222. <https://doi.org/10.1016/j.jallcom.2014.01.208>.
- (21) Tang, J.; Fabbri, J.; Robinson, R. D.; Zhu, Y.; Herman, I. P.; Steigerwald, M. L.; Brus, L. E. Solid-Solution Nanoparticles: Use of a Nonhydrolytic Sol–Gel Synthesis To Prepare HfO<sub>2</sub> and Hf<sub>x</sub>Zr<sub>1-x</sub>O<sub>2</sub> Nanocrystals. *Chem. Mater.* **2004**, *16* (7), 1336–1342. <https://doi.org/10.1021/cm049945w>.
- (22) Pucci, A.; Clavel, G.; Willinger, M.-G.; Zitoun, D.; Pinna, N. Transition Metal-Doped ZrO<sub>2</sub> and HfO<sub>2</sub> Nanocrystals. *J. Phys. Chem. C* **2009**, *113* (28), 12048–12058. <https://doi.org/10.1021/jp9029375>.
- (23) Armelao, L.; Bertagnolli, H.; Bleiner, D.; Groenewolt, M.; Gross, S.; Krishnan, V.; Sada, C.; Schubert, U.; Tondello, E.; Zattin, A. Highly Dispersed Mixed Zirconia and Hafnia Nanoparticles in a Silica Matrix: First Example of a ZrO<sub>2</sub>–HfO<sub>2</sub>–SiO<sub>2</sub> Ternary Oxide System. *Advanced Functional Materials* **2007**, *17* (10), 1671–1681. <https://doi.org/10.1002/adfm.200600458>.

- (24) Liu, M.; He, G.; Zhu, L. Q.; Fang, Q.; Li, G. H.; Zhang, L. D. Microstructure and Interfacial Properties of  $\text{HfO}_2\text{--Al}_2\text{O}_3$  Nanolaminate Films. *Applied Surface Science* **2006**, 252 (18), 6206–6211. <https://doi.org/10.1016/j.apsusc.2005.08.022>.
- (25) Cho, M.-H.; Roh, Y. S.; Whang, C. N.; Jeong, K.; Choi, H. J.; Nam, S. W.; Ko, D.-H.; Lee, J. H.; Lee, N. I.; Fujihara, K. Dielectric Characteristics of  $\text{Al}_2\text{O}_3\text{--HfO}_2$  Nanolaminates on Si(100). *Applied Physics Letters* **2002**, 81 (6), 1071. <https://doi.org/10.1063/1.1499223>.
- (26) Ylivaara, O. M. E.; Kilpi, L.; Liu, X.; Sintonen, S.; Ali, S.; Laitinen, M.; Julin, J.; Haimi, E.; Sajavaara, T.; Lipsanen, H.; Hannula, S.-P.; Ronkainen, H.; Puurunen, R. L. Aluminum Oxide/Titanium Dioxide Nanolaminates Grown by Atomic Layer Deposition: Growth and Mechanical Properties. *Journal of Vacuum Science & Technology A: Vacuum, Surfaces, and Films* **2016**, 35 (1), 01B105. <https://doi.org/10.1116/1.4966198>.
- (27) Jeon, S.; Yang, H.; Park, D.-G.; Hwang, H. Electrical and Structural Properties of Nanolaminate ( $\text{Al}_2\text{O}_3/\text{ZrO}_2/\text{Al}_2\text{O}_3$ ) for Metal Oxide Semiconductor Gate Dielectric Applications. *Japanese journal of applied physics* **2002**, 41 (4S), 2390.
- (28) Jeon, S.; Yang, H.; Chang, H. S.; Park, D.-G.; Hwang, H. Ultrathin Nitrided-Nanolaminate ( $\text{Al}_2\text{O}_3/\text{ZrO}_2/\text{Al}_2\text{O}_3$ ) for Metal–Oxide–Semiconductor Gate Dielectric Applications. *Journal of Vacuum Science & Technology B: Microelectronics and Nanometer Structures* **2002**, 20 (3), 1143. <https://doi.org/10.1116/1.1481864>.
- (29) Ding, S.-J.; Zhang, M.; Chen, W.; Zhang, D. W.; Wang, L.-K.; Wang, X. P.; Zhu, C.; Li, M.-F. High Density and Program-Erasable Metal-Insulator-Silicon Capacitor with a Dielectric Structure of  $\text{SiO}_2/\text{HfO}_2\text{--Al}_2\text{O}_3$  nanolaminate/ $\text{Al}_2\text{O}_3$ . *Applied Physics Letters* **2006**, 88 (4), 042905. <https://doi.org/10.1063/1.2168227>.
- (30) Hausmann, D. M.; Gordon, R. G. Surface Morphology and Crystallinity Control in the Atomic Layer Deposition (ALD) of Hafnium and Zirconium Oxide Thin Films. *Journal of Crystal Growth* **2003**, 249 (1–2), 251–261. [https://doi.org/10.1016/S0022-0248\(02\)02133-4](https://doi.org/10.1016/S0022-0248(02)02133-4).
- (31) Cho, D.-Y.; Jung, H. S.; Yu, I.-H.; Yoon, J. H.; Kim, H. K.; Lee, S. Y.; Jeon, S. H.; Han, S.; Kim, J. H.; Park, T. J.; Park, B.-G.; Hwang, C. S. Stabilization of Tetragonal  $\text{HfO}_2$  under Low Active Oxygen Source Environment in Atomic Layer Deposition. *Chem. Mater.* **2012**, 24 (18), 3534–3543. <https://doi.org/10.1021/cm3001199>.
- (32) Durrani, S. M. A. CO-Sensing Properties of Hafnium Oxide Thin Films Prepared by Electron Beam Evaporation. *Sensors and Actuators B: Chemical* **2007**, 120 (2), 700–705. <https://doi.org/10.1016/j.snb.2006.03.034>.
- (33) Karaduman, I.; Barin, Ö.; Yıldız, D. E.; Acar, S. The Effect of Ultraviolet Irradiation on the Ultra-Thin  $\text{HfO}_2$  Based CO Gas Sensor. *Journal of Applied Physics* **2015**, 118 (17), 174501. <https://doi.org/10.1063/1.4935139>.
- (34) Karaduman, I.; Acar, S. The Gas Sensing Properties of Hafnium Oxide Thin Films Depending on the Annealing Environment. *Mod. Phys. Lett. B* **2017**, 31 (30), 1750284. <https://doi.org/10.1142/S0217984917502840>.
- (35) Chen, H.-I.; Chang, C.-H.; Lu, H.-H.; Liu, I.-P.; Chen, W.-C.; Ke, B.-Y.; Liu, W.-C. Hydrogen Sensing Performance of a  $\text{Pd}/\text{HfO}_2/\text{GaN}$  Metal-Oxide-Semiconductor (MOS) Schottky Diode. *Sensors and Actuators B: Chemical* **2018**, 262, 852–859. <https://doi.org/10.1016/j.snb.2018.02.077>.

- (36) Böске, T. S.; Müller, J.; Bräuhаus, D.; Schröder, U.; Böttger, U. Ferroelectricity in Hafnium Oxide Thin Films. *Applied Physics Letters* **2011**, *99* (10), 102903. <https://doi.org/10.1063/1.3634052>.
- (37) Park, M. H.; Lee, Y. H.; Kim, H. J.; Kim, Y. J.; Moon, T.; Kim, K. D.; Müller, J.; Kersch, A.; Schroeder, U.; Mikolajick, T.; Hwang, C. S. Ferroelectricity and Antiferroelectricity of Doped Thin HfO<sub>2</sub>-Based Films. *Advanced Materials* **2015**, *27* (11), 1811–1831. <https://doi.org/10.1002/adma.201404531>.
- (38) Hoffmann, M.; Schroeder, U.; Schenk, T.; Shimizu, T.; Funakubo, H.; Sakata, O.; Pohl, D.; Drescher, M.; Adelman, C.; Materlik, R.; Kersch, A.; Mikolajick, T. Stabilizing the Ferroelectric Phase in Doped Hafnium Oxide. *Journal of Applied Physics* **2015**, *118* (7), 072006. <https://doi.org/10.1063/1.4927805>.
- (39) Abe, C.; Nakayama, S.; Shiokawa, M.; Kawashima, H.; Katayama, K.; Shiraishi, T.; Shimizu, T.; Funakubo, H.; Uchida, H. Crystal Structure and Dielectric/Ferroelectric Properties of CSD-Derived HfO<sub>2</sub>-ZrO<sub>2</sub> Solid Solution Films. *Ceramics International* **2017**, *43*, S501–S505. <https://doi.org/10.1016/j.ceramint.2017.05.253>.
- (40) Suntola, T. Atomic Layer Epitaxy. *Thin Solid Films* **1992**, *216* (1), 84–89. [https://doi.org/10.1016/0040-6090\(92\)90874-B](https://doi.org/10.1016/0040-6090(92)90874-B).
- (41) Miikkulainen, V.; Leskelä, M.; Ritala, M.; Puurunen, R. L. Crystallinity of Inorganic Films Grown by Atomic Layer Deposition: Overview and General Trends. *Journal of Applied Physics* **2013**, *113* (2), 021301. <https://doi.org/10.1063/1.4757907>.
- (42) Chaaya, A. A.; Viter, R.; Baleviciute, I.; Bechelany, M.; Ramanavicius, A.; Gertner, Z.; Erts, D.; Smyntyna, V.; Miele, P. Tuning Optical Properties of Al<sub>2</sub>O<sub>3</sub>/ZnO Nanolaminates Synthesized by Atomic Layer Deposition. *J. Phys. Chem. C* **2014**, *118* (7), 3811–3819. <https://doi.org/10.1021/jp411970w>.
- (43) Yamada, A.; Sang, B.; Konagai, M. Atomic Layer Deposition of ZnO Transparent Conducting Oxides. *Applied Surface Science* **1997**, *112*, 216–222. [https://doi.org/10.1016/S0169-4332\(96\)01022-7](https://doi.org/10.1016/S0169-4332(96)01022-7).
- (44) Hausmann, D. M.; de Rouffignac, P.; Smith, A.; Gordon, R.; Monsma, D. Highly Conformal Atomic Layer Deposition of Tantalum Oxide Using Alkylamide Precursors. *Thin Solid Films* **2003**, *443* (1–2), 1–4. [https://doi.org/10.1016/S0040-6090\(03\)00502-9](https://doi.org/10.1016/S0040-6090(03)00502-9).
- (45) Kukli, K.; Ritala, M.; Sajavaara, T.; Keinonen, J.; Leskelä, M. Atomic Layer Deposition of Hafnium Dioxide Films from Hafnium Tetrakis(Ethylmethanamide) and Water. *Chemical Vapor Deposition* **2002**, *8* (5), 199–204. [https://doi.org/10.1002/1521-3862\(20020903\)8:5<199::AID-CVDE199>3.0.CO;2-U](https://doi.org/10.1002/1521-3862(20020903)8:5<199::AID-CVDE199>3.0.CO;2-U).
- (46) Hackley, J. C.; Gougousi, T. Properties of Atomic Layer Deposited HfO<sub>2</sub> Thin Films. *Thin Solid Films* **2009**, *517* (24), 6576–6583. <https://doi.org/10.1016/j.tsf.2009.04.033>.
- (47) Kim, H.; McIntyre, P. C.; Saraswat, K. C. Effects of Crystallization on the Electrical Properties of Ultrathin HfO<sub>2</sub> Dielectrics Grown by Atomic Layer Deposition. *Applied Physics Letters* **2003**, *82* (1), 106–108. <https://doi.org/10.1063/1.1533117>.
- (48) Kukli, K.; Ritala, M.; Lu, J.; Haärsta, A.; Leskelä, M. Properties of HfO<sub>2</sub> Thin Films Grown by ALD from Hafnium Tetrakis(Ethylmethanamide) and Water. *J. Electrochem. Soc.* **2004**, *151* (8), F189. <https://doi.org/10.1149/1.1770934>.
- (49) Gusev, E. P.; Cabral, C.; Copel, M.; D’Emic, C.; Gribelyuk, M. Ultrathin HfO<sub>2</sub> Films Grown on Silicon by Atomic Layer Deposition for Advanced Gate Dielectrics Applications. *Microelectronic Engineering* **2003**, *69* (2), 145–151. [https://doi.org/10.1016/S0167-9317\(03\)00291-0](https://doi.org/10.1016/S0167-9317(03)00291-0).

- (50) Cady, W. A.; Varadarajan, M. RCA Clean Replacement. *Journal of The Electrochemical Society* **1996**, *143* (6), 2064–2067.
- (51) Ye, L.; Kropp, J. A.; Gougousi, T. In Situ Infrared Spectroscopy Study of the Surface Reactions during the Atomic Layer Deposition of TiO<sub>2</sub> on GaAs (100) Surfaces. *Applied Surface Science* **2017**, *422*, 666–674. <https://doi.org/10.1016/j.apsusc.2017.05.264>.
- (52) Hackley, J. C.; Demaree, J. D.; Gougousi, T. Interface of Atomic Layer Deposited HfO<sub>2</sub> Films on GaAs (100) Surfaces. *Applied Physics Letters* **2008**, *92* (16), 162902. <https://doi.org/10.1063/1.2908223>.
- (53) Gougousi, T.; Hackley, J. C.; Demaree, J. D.; Lacis, J. W. Growth and Interface Evolution of HfO<sub>2</sub> Films on GaAs(100) Surfaces. *Journal of The Electrochemical Society* **2010**, *157* (5), H551–H556. <https://doi.org/10.1149/1.3353166>.
- (54) Ye, L.; Gougousi, T. In Situ Infrared Spectroscopy Study of the Interface Self-Cleaning during the Atomic Layer Deposition of HfO<sub>2</sub> on GaAs(100) Surfaces. *Applied Physics Letters* **2014**, *105* (12), 121604. <https://doi.org/10.1063/1.4896501>.
- (55) Timm, R.; Fian, A.; Hjort, M.; Thelander, C.; Lind, E.; Andersen, J. N.; Wernersson, L.-E.; Mikkelsen, A. Reduction of Native Oxides on InAs by Atomic Layer Deposited Al<sub>2</sub>O<sub>3</sub> and HfO<sub>2</sub>. *Applied Physics Letters* **2010**, *97* (13), 132904. <https://doi.org/10.1063/1.3495776>.
- (56) Timm, R.; Head, A. R.; Yngman, S.; Knutsson, J. V.; Hjort, M.; McKibbin, S. R.; Troian, A.; Persson, O.; Urpelainen, S.; Knudsen, J.; Schnadt, J.; Mikkelsen, A. Self-Cleaning and Surface Chemical Reactions during Hafnium Dioxide Atomic Layer Deposition on Indium Arsenide. *Nature Communications* **2018**, *9* (1), 1412. <https://doi.org/10.1038/s41467-018-03855-z>.
- (57) Chang, C.-H.; Chiou, Y.-K.; Chang, Y.-C.; Lee, K.-Y.; Lin, T.-D.; Wu, T.-B.; Hong, M.; Kwo, J. Interfacial Self-Cleaning in Atomic Layer Deposition of HfO<sub>2</sub> Gate Dielectric on In<sub>0.15</sub>Ga<sub>0.85</sub>As. *Applied Physics Letters* **2006**, *89* (24), 242911. <https://doi.org/10.1063/1.2405387>.
- (58) Kobayashi, M.; Chen, P. T.; Sun, Y.; Goel, N.; Majhi, P.; Garner, M.; Tsai, W.; Pianetta, P.; Nishi, Y. Synchrotron Radiation Photoemission Spectroscopic Study of Band Offsets and Interface Self-Cleaning by Atomic Layer Deposited HfO<sub>2</sub> on In<sub>0.53</sub>Ga<sub>0.47</sub>As and In<sub>0.52</sub>Al<sub>0.48</sub>As. *Applied Physics Letters* **2008**, *93* (18), 182103. <https://doi.org/10.1063/1.3020298>.
- (59) Kang, Y.-S.; Kim, D.-K.; Jeong, K.-S.; Cho, M.-H.; Kim, C. Y.; Chung, K.-B.; Kim, H.; Kim, D.-C. Structural Evolution and the Control of Defects in Atomic Layer Deposited HfO<sub>2</sub>–Al<sub>2</sub>O<sub>3</sub> Stacked Films on GaAs. *ACS Applied Materials & Interfaces* **2013**, *5* (6), 1982–1989. <https://doi.org/10.1021/am302803f>.
- (60) Hinkle, C. L.; Sonnet, A. M.; Vogel, E. M.; McDonnell, S.; Hughes, G. J.; Milojevic, M.; Lee, B.; Aguirre-Tostado, F. S.; Choi, K. J.; Kim, H. C.; Kim, J.; Wallace, R. M. GaAs Interfacial Self-Cleaning by Atomic Layer Deposition. *Applied Physics Letters* **2008**, *92* (7), 071901. <https://doi.org/10.1063/1.2883956>.
- (61) Henegar, A. J.; Cook, A. J.; Dang, P.; Gougousi, T. Native Oxide Transport and Removal During Atomic Layer Deposition of TiO<sub>2</sub> Films on GaAs(100) Surfaces. *ACS Appl. Mater. Interfaces* **2016**, *8* (3), 1667–1675. <https://doi.org/10.1021/acsami.5b08998>.
- (62) Ye, L.; Gougousi, T. Indium Diffusion and Native Oxide Removal during the Atomic Layer Deposition (ALD) of TiO<sub>2</sub> Films on InAs(100) Surfaces. *ACS Appl. Mater. Interfaces* **2013**, *5* (16), 8081–8087. <https://doi.org/10.1021/am402161f>.

- (63) Rim, Y. S.; Bae, S.-H.; Chen, H.; Marco, N. D.; Yang, Y. Recent Progress in Materials and Devices toward Printable and Flexible Sensors. *Advanced Materials* **2016**, 28 (22), 4415–4440. <https://doi.org/10.1002/adma.201505118>.
- (64) Jeong, S.; Moon, J. Low-Temperature, Solution-Processed Metal Oxide Thin Film Transistors. *J. Mater. Chem.* **2011**, 22 (4), 1243–1250. <https://doi.org/10.1039/C1JM14452A>.